

1 **Ailanthone inhibits cell growth and migration of cisplatin-resistant bladder cancer cells**
2 **through down-regulation of Nrf2, YAP and c-Myc expression.**

3
4 Martina Daga^{a, 1}, Stefania Pizzimenti^{a, 1,*}, Chiara Dianzani^b, Marie Angele Cucci^a, Roberta Cavalli^b,
5 Margherita Grattarola^a, Benedetta Ferrara^b, Francesco Trotta^{c, 2} and Giuseppina Barrera^{a, 2}

6 ^a Department of Clinical and Biological Science, University of Turin, Corso Raffaello 30, 10125
7 Torino, (Italy)

8 ^b Department of Drug Science and Technology, University of Turin, Via Pietro Giuria 9, 10125
9 Turin, Italy

10 ^c Department of Chemistry, University of Turin, Via Pietro Giuria 7, 10125 Turin, Italy

11
12 ¹ Martina Daga and Stefania Pizzimenti contributed equally to this work.

13
14 *Corresponding Author

15 Stefania Pizzimenti, Department of Clinical and Biological Science, University of Turin, Corso
16 Raffaello 30, 10125 Torino, (Italy)

17 Tel: +39-011-6707792; Fax: +39-011-6707753

18 Mail: stefania.pizzimenti@unito.it

19
20 ² Co-last authors.

21
22
23
24
25
26
27
28
29
30
31
32
33
34
35
36
37
38
39
40
41
42
43
44
45
46
47
48
49
50 **WORD COUNT: 4.972**

51 **Abstract**

52 **Background:** Ailanthone (Aila) is a natural active compound isolated from the *Ailanthus altissima*,
53 which has been shown to possess an “in vitro” growth-inhibitory effect against several cancer cell
54 lines. Advanced bladder cancer is a common disease characterized by a frequent onset of resistance
55 to cisplatin-based therapy. The cisplatin (CDDP) resistance is accompanied by an increase in Nrf2
56 protein expression which contributes to conferring resistance. Recently, we demonstrated a cross-
57 talk between Nrf2 and YAP. YAP has also been demonstrated to play an important role in
58 chemoresistance of bladder cancer.

59 **Purpose:** We analyzed the antitumor effect of Aila in sensitive and CDDP-resistant bladder cancer
60 cells and the molecular mechanisms involved in Aila activity.

61 **Study design:** Sensitive and CDDP-resistant 253J B-V and 253J bladder cancer cells, and
62 intrinsically CDDP-resistant T24 bladder cancer cells were used. Cells were treated with diverse
63 concentrations of Aila and proliferation, cell cycle, apoptosis and gene expressions were
64 determined.

65 **Methods:** Aila toxicity and proliferation were determined by MTT and colony forming methods,
66 respectively. Cell cycle was determined at cytofluorimeter by PI staining method. Apoptosis was
67 detected using Annexin V and PI double staining followed by quantitative flow cytometry.

68 Expressions of Nrf2, Yap, c-Myc, and house-keeping genes were determined by western blot with
69 specific antibodies. Cell migration was detected by wound healing and Boyden chamber analysis.

70 **Results:** Aila inhibited growth of sensitive and CDDP-resistant bladder cancer cells with the same
71 effectiveness, and reduced cell migration with higher effectiveness in CDDP resistant cells.

72 Interestingly, Aila strongly reduced Nrf2 expression in all cell lines. Cell cycle analysis revealed an
73 accumulation of Aila-treated cells in G0/G1 phase. Moreover, Aila significantly reduced YAP and
74 c-Myc protein expression. The random and the oriented migration were strongly inhibited by Aila
75 treatment, in particular in CDDP-resistant cells.

76 **Conclusions:** Aila, inhibited proliferation and invasiveness of bladder cancer cells. Its high
77 effectiveness in CDDP resistant cells could be related to the inhibition of Nrf2 , YAP and c-Myc
78 expressions. Aila could represent a new tool to overcome CDDP resistance in bladder cancer.

79
80 **Keywords:** Ailanthone; bladder cancer; CDDP-resistance; Nrf2; Yap; c-Myc.

81
82 **Abbreviation:** Aila, Ailanthone; CDDP, Cisplatin; Nrf2, NF-E2-related factor 2; YAP, yes-
83 associated protein; MTT, 3-(4,5-Dimethylthiazol-2-yl)-2,5-diphenyltetrazolium bromide; Keap1,
84 Kelch-like ECH-associated protein 1; ARE, antioxidant response element; EpRE, electrophile
85 response element; RPMI 1640, Roswell Park Memorial Institute medium; FBS, fetal bovine serum;
86 EDTA: Ethylenediaminetetraacetic acid; SDS, sodium dodecyl sulfate; TBS: tris-buffered saline;
87 GAPDH, glyceraldehyde 3 phosphate dehydrogenase; GSTA4, Glutathione S-transferase A4; PI,
88 propidium iodide, FITC, fluorescein isothiocyanate;

101 **Introduction**

102 Ailanthone (Aila) [(1 β ,11 β ,12 α)-11,20-Epoxy-1,11,12-trihydroxypicrasa-3,13(21)-diene-2,16-
103 dione] is a natural active compound isolated from the plant *Ailanthus altissima* (Bray et al., 1987).
104 Aila has a wide spectrum of biological activities, it is traditionally used to treat ascariasis, diarrhoea,
105 spermatorrhoea, bleeding and gastrointestinal diseases, and it has been found to have anti-
106 inflammatory activity (Kim et al., 2015). Aila has been shown to possess an “in vitro” growth-
107 inhibitory effect against several cancer cell lines (Wang R. et al., 2016), but the mechanisms
108 involved in the antiproliferative activity of Aila are not completely elucidated and they seem to be
109 related to the cancer cell type. Indeed, in some cell models Aila induced G0/G1-phase cell cycle
110 arrest, and triggered DNA damage and apoptosis pathway (Zhuo et al., 2015), in others, Aila
111 induced G2/M phase cell cycle arrest and an apoptosis through downregulation of Bcl2 and
112 upregulation of Bax (Chen Y et al., 2017). Ni et al. (2017) found that Aila inhibited the growth of
113 several lung cancer cells through repression of DNA replication via RPA1 down regulation. He et
114 al. (2016) demonstrated that Aila was a potent inhibitor of androgen receptor and it was able to
115 overcome resistance in castration-resistant cancer cells through the binding with the co-chaperone
116 p23 protein.

117 Urothelial carcinoma of the bladder is a common malignancy in men. At the initial diagnosis, about
118 30% of tumors have already infiltrated the bladder muscle wall and are classified as muscle-invasive
119 bladder cancers. Muscle-invasive bladder cancer is associated with poor prognosis. Standard of care
120 for muscle-invasive bladder cancer is cystectomy combined with platinum-based chemotherapy
121 regimens (Madersbacher et al., 2003). The clinical benefit of cisplatin-based chemotherapy is
122 limited and the majority of the patients eventually develop cisplatin-resistant disease (Shah et al.,
123 2011). Thus, the identification of novel agents able to overcome this resistant disease is an urgent
124 and unmet need.

125 In bladder cancer cells, we previously demonstrated that the CDDP resistance was accompanied by
126 an increase in Nrf2 (NF-E2-related factor 2) protein expressions which contributes to conferring
127 CDDP resistance (Ciamporcero et al., 2018). The transcription factor Nrf2 is the master regulator of
128 antioxidant and cytoprotective genes (Rojo de la Vega et al., 2018). It is present in the cytoplasm
129 bound to Keap1 (Kelch-like ECH-associated protein 1) which, by forming a complex with Cul3
130 and Rbx1, and this E3 ubiquitin ligase complex, is able to ubiquitinate Nrf2, resulting in Nrf2
131 proteasomal degradation. In response to an increase of oxidative stress, the cysteine residues of
132 Keap1 become oxidized, resulting in a conformational change of the Keap1–Nrf2 complex which
133 prevents Nrf2 ubiquitination (Itoh et al., 2004). As a consequence, Nrf2 accumulates in nuclei,
134 and after heterodimerization with Maf proteins, binds antioxidant response element
135 (ARE)/electrophile response element (EpRE) and activates target genes for cytoprotection (Itoh et
136 al., 2004). Due to its cytoprotective role, the Nrf2 increase in resistant cells has been proposed as
137 an important tool for maintaining drug resistance (No et al, 2014). Indeed, Nrf2 overexpression is
138 associated with clinically relevant CDDP resistance in bladder cancer patients (Hayden et al., 2014).
139 Recently, in bladder cancer cells, we demonstrated a cross-talk between Nrf2 and Yap: Nrf2
140 silencing and glutathione depletion reduced YAP expression, possibly through the inhibition of
141 GABP transcriptional activity (Ciamporcero et al., 2018). Moreover, YAP protein is also involved
142 in maintaining antioxidant capacity: the stimulation of YAP prevents, whereas the down-regulation
143 of YAP promotes oxidative stress-induced cell death in cardiomyocytes (Tao et al., 2016).

144 Increasing evidence has demonstrated the involvement of YAP in chemoresistance of several types
145 of cancers. YAP, is a key component of the Hippo tumor-suppressor pathway (Harvey et al., 2013).
146 Hippo pathway-mediated YAP phosphorylation on Ser127 leads to its cytoplasm sequestration or
147 ubiquitination and degradation (Zhao et al., 2010). Conversely, unphosphorylated YAP translocates
148 into the nucleus where it binds to the TEAD transcription factor, triggering the expression of several
149 downstream transcriptional targets involved in organ size control, cell proliferation, migration and
150 survival, such as c-Myc, cyr 61 and survivin. Indeed, YAP expression inhibition results in reduced

61
62
63
64
65

151 cell proliferation and increased cell death (Zhao et al., 2008). YAP expression and nuclear
152 localization strongly correlate with poor patient outcome and the progression of several tumors,
153 including bladder cancer (Liu et al., 2013). The constitutive expression and activation of YAP was
154 inversely correlated with *in vitro* and *in vivo* CDDP sensitivity of urothelial cell carcinoma cells:
155 YAP overexpression protects, while YAP knockdown sensitizes cancer cells to chemotherapy and
156 radiation effects via increased accumulation of DNA damage and apoptosis (Ciamporcero et al.,
157 2016). Moreover, the knockdown of YAP and the silencing of Nrf2 enhanced sensitivity of bladder
158 cancer cells to CDDP and reduced their migration (Ciamporcero et al., 2018).
159 Aila has been demonstrated to exhibit *in vitro* growth-inhibitory effects against several cancer cell
160 lines. However, the antitumor activity in bladder cancer cells, sensitive and resistant to CDDP
161 treatment, remains to be elucidated. In this paper we demonstrated, for the first time, that Aila is
162 able to inhibit proliferation and migration in these cell models, in particular in CDDP resistant cells,
163 and that these effects could be linked to its ability to inhibit Nrf2, Yap and Myc expressions.

164

165 **Materials and Methods**

166

167 *Cells and culture conditions*

168 253J B-V and 253J cell lines were kindly provided by Dr Colin Dinney (MD Anderson Cancer
169 Center). Human cell line T24 was purchased from ATCC (Manassas, VA, USA). These cells were
170 cultured in RPMI 1640, supplemented with 10% FBS, 100 units per ml penicillin and 100µg/ml
171 streptomycin in a 5% CO₂, 37°C incubator. The CDDP resistance in 253J B-V and 253J was
172 induced and maintained as previously described (Ciamporcero et al., 2018).

173

174 *MTT assay*

175 The toxic effect of Aila was determined through the 3-(4,5-dimethyl thiazol-2-yl)-2,5-
176 diphenyltetrazolium bromide (MTT) assay as previously described (Ciamporcero et al., 2018). This
177 colorimetric assay may be interpreted as a measure of both cell viability and cell proliferation
178 (Sylvester, 2011). Cells were seeded (800–1500 cells/well) in 200 µl of serum-supplemented
179 medium and treated with different concentrations of Aila (Baoji Herbest Bio-Tech Co., Ltd., Baoji
180 city Shannxi Provence China). To confirm the CDDP resistance, CDDP was added at the
181 concentrations ranging from 0.1 to 1 µg/ml. Untreated cells were used as control. After 72 hours,
182 the drug was removed and MTT assay was performed.

183

184 *Colony-forming assay*

185 Cells were trypsinized, washed in 1× PBS, and seeded (500 cells/well) into a six-well plate and left
186 overnight to attach. After 24 h, the cells were treated with the compounds and the medium was
187 changed after 72 h. Cells were cultured for 9–11 days and subsequently fixed and stained with a
188 solution of 90% crystal violet (Sigma–Aldrich), 10% methanol.

189

190 *Lysate preparation and western blot analysis*

191 Lysate preparation and western blot analysis were performed as previously described (Ciampocero
192 et al., 2018). Antibodies used were as follows: glyceraldehyde 3 phosphate dehydrogenase
193 (GAPDH) (#5174) (Cell Signaling, Boston, MA, USA); β-actin (sc-47778), YAP (sc15407), Nrf2
194 (sc 722), α-tubulin (04-1117, Millipore, Billerica, MA, USA); c-Myc (clone 9E10, sc 40, Santa
195 Cruz Biotechnology, CA), GSTA4 (Glutathione S-transferase A4) (SAB1401164, Sigma–
196 Aldrich). The detection of the bands was carried out after reaction with chemiluminescence reagents
197 (PerkinElmer NEL105001EA) through film (Santa Cruz Biotechnology sc-201697)
198 autoradiography.

199

200 *Cytofluorimetric analysis*

201

202

203

204

205

201 Adherent and non-adherent treated and control cells were harvested 24 hours after the treatment
202 with 0.5 and 1 $\mu\text{g/ml}$ of Aila. Cells were washed with 1X PBS, fixed in 70% cold ethanol,
203 resuspended in a buffer containing 0.02 mg/ml RNase A (Worthington), 0.05 mg/ml propidium
204 iodide (PI) (Sigma–Aldrich), 0.2% v/v Nonidet P-40 (Sigma–Aldrich), 0.1% w/v sodium citrate
205 (Sigma–Aldrich), and analyzed with a FACScan cytometer (Becton Dickinson, Accuri). For
206 apoptosis analysis 1×10^6 cells were harvested and stained with FITC-Annexin 5 and PI according to
207 the manufacturer protocol (FITC Annexin V Apoptosis Detection Kit (BD Biosciences Cat N°
208 556547).

209 210 *Cell motility assay*

211 In the wound-healing assay, after starvation for 18–24 h in serum-free medium, cells were plated
212 onto six-well plates (10^6 cell/well) and grown to confluence. Cell monolayers were wounded by
213 scratching with a pipette tip along the diameter of the well, and they were washed twice with serum-
214 free medium before their incubation with diverse concentrations of Aila (0.01, 0.05 and 0.1 $\mu\text{g/ml}$).
215 In order to monitor cell movement into the wounded area, five fields of each wound were
216 photographed immediately after the scratch (T0) and after 24 hours (Dianzani et al., 2014). The
217 endpoint of the assay was measured by calculating the reduction in the width of the wound after 24
218 hours and compared to T0 which is set at 100%. The area of wound healing was calculated by
219 using the ImageJ software (Schneider et al., 2012). In the Boyden chamber (BD Biosciences, San
220 Jose, CA) invasion assay, cells (2000) were plated onto the apical side of 50 $\mu\text{g mL}^{-1}$ Matrigel-
221 coated filters (8.2 mm diameter and 0.5 μm pore size; Neuro Probe, Inc.; BIOMAP snc, Milan,
222 Italy) in serum-free medium with or without increasing concentration of the Aila (0.01, 0.05 and 0.1
223 $\mu\text{g/ml}$). Medium containing 20% FCS was placed in the basolateral chamber as a chemo attractant.
224 After 24 hours, cells on the apical side were wiped off with Q-tips. Cells on the bottom of the filter
225 were stained with crystal violet and counted (five fields of each triplicate filter) with an inverted
226 microscope.

227 228 *Statistical analysis*

229 Data were expressed as means \pm SD. Significance between experimental groups was determined by
230 one-way ANOVA followed by the Bonferroni multiple comparison post-test using GraphPad InStat
231 software (San Diego, CA, USA). Values of $p \leq 0.05$ were considered statistically significant.

232 233 **Results**

234 *Aila effect on bladder cancer cell growth and colony forming.*

235 To analyze the ability of Aila to affect cell growth and colony forming of sensitive and CDDP-
236 resistant bladder cancer cells, 253J B-V and 253J B-V resistant to CDDP (253J B-V C-r), 253J and
237 253J resistant to CDDP (253J C-r), and T24 (intrinsically CDDP resistant) cells were exposed to
238 different doses of Aila. Results obtained demonstrated that the Aila was more effective than CDDP
239 in reducing cell growth of 253J B-V cells and, in particular, Aila reduced the growth of 253J B-V
240 C-r cells to the same extent as the sensitive cells (Fig. 1A). Colony forming assay confirmed the
241 effectiveness of Aila treatment in sensitive and CDDP resistant 253J B-V cells (Fig. 1B).

242 The cytotoxic and antiproliferative effect of Aila was demonstrated in 253J cells, also (Fig. 2). The
243 reduction of proliferation after 72 hours from the treatment with 0.5 and 1 $\mu\text{g/ml}$ of Aila was similar
244 in sensitive and CDDP resistant cells (Fig. 2A). The colony forming assay also confirmed the
245 effectiveness of Aila in 253J C-r cells (Fig. 2B). The third cell line employed in our experiments
246 was the T24 cells. This cell line has been demonstrated to be resistant not only to CDDP but also to
247 other DNA damaging agents such as the anthracycline antibiotic doxorubicin and the Podophyllum
248 peltatum toxin etoposide (Ciamporcero et al., 2016). Analogously, to that observed in the previous

59
60
61
62
63
64
65

249 cell lines, Aila reduced T24 cell growth and colony forming to a higher extent than CDDP (Fig.3
250 A, B).

251 252 *Aila effects on Nrf2 and Nrf2 target gene expressions*

253 We previously demonstrated that Nrf2 expression is higher in CDDP-resistant bladder cancer cells
254 than in sensitive cells and that the silencing of Nrf2 in CDDP resistant bladder cancer cells, can
255 sensitize them to CDDP and reduce cell viability (Ciamporcerro et al., 2018). Since the Aila
256 treatment reduced proliferation and colony forming of CDDP resistant cells to the same extent as
257 the sensitive cells, we analyzed whether Aila could reduce Nrf2 expression in these cell lines. The
258 analysis were performed after 24 and 48 hours from the treatment. Results demonstrated that Nrf2
259 expression was inhibited until 48 hours in a dose dependent way in both sensitive and resistant
260 bladder cancer cells (Fig. 4 A,B). The reduction of Nrf2 protein was confirmed by the contemporary
261 reduction of GSTA4, a Nrf2 target gene (Fig 5 A,B).

262 263 *Effect of Aila on cell cycle and apoptosis of bladder cancer cells*

264 To deepen the antiproliferative activity by Aila we performed the analysis of cell cycle and
265 apoptosis in sensitive and CDDP-resistant 253J B-V cells. In both cell lines, Aila (from 0.1 to 1
266 $\mu\text{g/ml}$) induced a significant increase in G0/G1 cells (Fig. 6 A,B), whereas treatments with the same
267 concentrations of Aila did not induce increase of apoptotic cells (data not shown).

268 269 *Aila inhibits YAP and c-Myc protein expression*

270 On the basis of our previous results that indicated a cross-talk between Nrf2 and YAP expression,
271 we analyzed in 253J B-V and 253J B-V C-r the expression of YAP. Moreover, since Myc and
272 YAP-TEAD integrate mitogenic and mechanical cues at the transcriptional level to control cell
273 proliferation (Croci et al., 2017), c-Myc protein expression was also examined. Results obtained
274 demonstrated that Aila inhibited YAP and c-Myc expression, both in sensitive and, particularly, in
275 resistant cell lines, which express YAP at high levels (Fig.7 A,B). The inhibition was dose-
276 dependent and persisted until 48 hours from the treatment.

277 278 *Effects of Aila on migration of bladder cancer cells*

279 YAP and Nrf2 also control the migration of cancer cells (Rojo de la Vega et al., 2018) which
280 contributes to their metastatic properties. Since Aila inhibited the expression of both Nrf2 and YAP
281 proteins, we analyzed its effect on cell migration. Cell motility was initially assessed using a wound
282 healing assay evaluating random cell migration in the presence or absence of diverse concentrations
283 of Aila (from 0.01 to 0.1 $\mu\text{g/ml}$). Analysis of the cell ability to migrate into the scratch showed that
284 Aila inhibited migration of both cell lines (Fig. 8 A,B) in a dose-dependent way. However, the
285 effect in CDDP-resistant cells was higher than in sensitive cells. Then, cell motility was assessed
286 using a Boyden chamber assay assessing directional migration and invasion of cells. Results
287 showed that Aila inhibited 253J B-V and 253J B-V C-r cell invasion in a concentration dependent
288 way in both cell lines, but, interestingly, the invasion of the CDDP-resistant cells was affected at
289 higher levels than the sensitive cells (Fig. 9). Control invasion was 72 ± 5 cells per wells for 253J B-
290 V and 84 ± 4 for 253J B-V C-r. Data are shown as percentages of inhibition versus the control
291 invasion measured on untreated cells. In both migration assays, doses and timing of treatments
292 minimized the possible confounding effects due to the Aila effect on cell growth.

293 294 **Discussion**

295 In the present study, Aila was found to be able to inhibit the proliferation of sensitive and CDDP
296 resistant bladder cancer cells with the same effectiveness. The inhibition of proliferation mostly
297 depended on the accumulation of cells in G0/G1 cell cycle phase of cell cycle, which, in turn, could
298 be dependent on the Nrf2, Yap and c-Myc down-regulation. Nrf2 and YAP expression are increased

61
62
63
64
65

299 in resistant cells (Ciamporcerro et al, 2016; Ciamporcerro et al., 2018) and both play an important
300 role in reducing proliferative capacity of cells. Beside the canonical Nrf2 role in orchestrating
301 antioxidant response, accumulating evidence has established that Nrf2 sustained proliferative
302 signaling and that its reduction correlated with a reduction of cell proliferation (Rojo de la Vega et
303 al., 2018). As a consequence, the down regulation of Nrf2 expression by Aila, could reduce the
304 cytoprotective role of Nrf2, thus facilitating its own antiproliferative action. Another naturally
305 occurring quassonoid, brusatol, extracted from the aerial parts of the *Brucea javanica* plant, has
306 been shown to inhibit Nrf2 and to sensitize cancer cells to several chemotherapeutic drugs (Ren et
307 al., 2011). However, the brusatol-mediated inhibition of Nrf2 was transient, persisting only 8 hours
308 from the treatment (Olayanju A et al., 2015). On the contrary, we demonstrated that after 48
309 hours the reduction of Nrf2 expression by Aila was still present, as well as the reduction of the
310 Nrf2 target gene GSTA4. The high antiproliferative effect of Aila in CDDP-resistant cells could be
311 sustained not only by this persistent inhibition of Nrf2 expression, but also by the contemporary
312 inhibition of YAP and Myc expression. Indeed YAP, through the activation of TEAD transcription
313 factors, has been demonstrated to be implicated in the control of growth, oncogenic transformation,
314 and epithelial-mesenchymal transition (Zao et al, 2008). Moreover, the binding of YAP with
315 TEADs upregulates the expression of several growth promoting factors, among those is the well
316 known oncogene c-myc (Neto- Silva et al., 2010). C-Myc and YAP-TEAD integrate mitogenic and
317 mechanical cues at the transcriptional level to control cell proliferation and cell cycle entry (Croci
318 et al., 2017).

319 Traditionally, the cytotoxic effect of platinum compounds depend on the formation of intrastrand
320 DNA cross-links [mostly double-strand breaks (DSB)], that lead to G2 arrest, apoptosis induction
321 and generation of oxidative stress (Yu et al., 2018). In this study we demonstrated that Aila
322 affected cell growth through mechanisms other than cisplatin. In our cell models, Aila induced a
323 cell cycle arrest in G0/G1 cells which can be in relation with the inhibition of YAP and c-Myc
324 expression. Moreover, no evidence of apoptosis induction was present, even after the treatment
325 with the highest Aila concentration. Thus, apoptosis seems not be involved in the reduction of cell
326 growth.

327 Another important effect displayed by low doses of Aila regarded the inhibition of both random and
328 directional migration. In determining this inhibitory effect, different pathways can be involved, in
329 which both Nrf2 and YAP play an important role (Zhang et al., 2016; Warren et al., 2018).

330 In cancer cell lines, Nrf2 promoted the epithelial mesenchymal transition by down-regulation of E-
331 cadherin, and Nrf2 knock-down greatly impaired migration and invasion (Rojo de la Vega et al.,
332 2018). For its part, YAP also is involved in cell invasion, since it induced epithelial mesenchymal
333 transition in cancer cells and YAP knock-down rescued the expression of epithelial markers (Zhao
334 et al., 2008).

335 336 **Conclusions**

337 Our results demonstrated, for the first time, that Aila inhibited proliferation and migration of
338 bladder cancer cells, by reducing Nrf2, YAP and c-Myc expression. Importantly, this effect was
339 displayed in CDDP-resistant cancer cells in which the down-regulation of Nrf2 and YAP
340 expressions was required to overcome the resistance. Since CDDP resistance is a common feature
341 in muscle invasive urothelial carcinoma of the bladder after platinum-based chemotherapy (Shah et
342 al., 2011), the identification of a novel agent able to overcome this resistant disease is of great
343 interest. From this point of view, Aila demonstrated favourable drug-like properties due to its good
344 bioavailability, high solubility and low hepatotoxicity (He et al, 2015).

345 In conclusion our results suggest that Aila may represent an important tool in the therapy of CDDP-
346 resistant bladder cancer and pave the way for further investigation in this field.

347
59
60
61
62
63
64
65

348 **Acknowledgments:** This work was supported by the University of Torino “ Ricerca Locale “ex
349 60%” Department of Clinical and Biological Sciences (BARG-RILO-16-01 and PIZS-RILO- 17-
350 01), Ricerca Locale “ex 60%” Department of Sciences and Pharmaceutical Technology (DIAC-
351 RILO-16-01 and DIAC-RILO-17-01), and CRT 2016 (TROFCRT1602).

352 **Conflict of interest**

353 The authors declare no conflict of interest.

354
355 **References**

356 Bray, D.H., Boardman, P., O'Neill, M.J., Chan, K.L., Phillipson, J.D., Warhurst, D.C., Suffness, M.,
357 1987. Plants as a source of antimalarial drugs 5. Activities of *Ailanthus altissima* stem constituents
358 and of some related quassinoids. *Phytother. Res.* 1, 22–24.

359
360 Chen, Y., Zhu, L., Yang, X., Wei, C., Chen, C., He, Y., Ji, Z., 2017. Ailanthone induces G2/M cell
361 cycle arrest and apoptosis of SGC-7901 human gastric cancer cells. *Mol Med Rep.* 16, 6821-6827.

362
363 Ciamporcero, E., Shen , H., Ramakrishnan, S., Yu Ku, S., Chintala, S., Shen, L., Adelaiye, R.,
364 Miles, K.M., Ullio, C., Pizzimenti, S., Daga, M., Azabdaftari, G., Attwood, K., Johnson, C., Zhang,
365 J., Barrera, G., Pili, R., 2016. YAP activation protects urothelial cell carcinoma from treatment-
366 induced DNA damage. *Oncogene.* 35, 1541-1553.

367
368 Ciamporcero, E., Daga, M., Pizzimenti, S., Roetto, A., Dianzani, C., Compagnone, A., Palmieri ,A.,
369 Ullio, C., Cangemi, L., Pili, R., Barrera, G., 2018. Crosstalk between Nrf2 and YAP contributes to
370 maintaining the antioxidant potential and chemoresistance in bladder cancer. *Free Radic Biol Med.*
371 115, 447-457.

372
373 Croci, O., De Fazio, S., Biagioni, F., Donato, E., Caganova, M., Curti, L., Doni, M., Sberna, S.,
374 Aldeghi, D., Biancotto, C., Verrecchia, A., Olivero, D., Amati, B., Campaner, S., 2017.
375 Transcriptional integration of mitogenic and mechanical signals by Myc and YAP. *Genes Dev.* 31,
376 2017-2022.

377
378 Dianzani, C., Minelli, R., Gigliotti, C.L., Occhipinti, S., Giovarelli, M., Conti, L., Boggio, E.,
379 Shivakumar, Y., Baldanzi, G., Malacarne, V., Orilieri, E., Cappellano, G., Fantozzi, R., Sblattero,
380 D., Yagi, J., Rojo, J.M., Chiocchetti, A., Dianzani, U., 2014. B7h triggering inhibits the migration
381 of tumor cell lines. *J Immunol.* 192, 4921-4931.

382
383 Harvey, K.F., Zhang, X., Thomas, D.M., 2013. The Hippo pathway and human cancer. *Nat Rev*
384 *Cancer* 13, 246–257.

385
386 Hayden, A., Douglas, J., Sommerlad, M., Andrews, L., Gould, K., Hussain, S., Thomas, G.J.,
387 Packham, G., Crabb, S.J., 2014. The Nrf2 transcription factor contributes to resistance to cisplatin
388 in bladder cancer. *Urol Oncol.* 32, 806-814.

389
390 He, Y., Peng, S., Wang, J., Chen, H., Cong, X., Chen, A., Hu, M., Qin, M., Wu, H., Gao, S., Wang,
391 L., Wang, X., Yi, Z., Liu, M., 2016. Ailanthone targets p23 to overcome MDV3100 resistance in
392 castration-resistant prostate cancer. *Nat Commun.* 7, 13122. <http://doi.org/10.1038/ncomms13122>

393
394 Itoh, K., Tong, KI., Yamamoto, M., 2004. Molecular mechanism activating Nrf2-Keap1 pathway in
395 regulation of adaptive response to electrophiles. *Free Radic Biol Med.* 36, 1208–1213.

396
60
61
62
63
64
65

- 397 Kim, H.M., Kim, S.J., Kim, H.Y., Ryu, B., Kwak, H., Hur, J., Choi, J.H., Jang, D.S., 2015.
398 Constituents of the stem barks of *Ailanthus altissima* and their potential to inhibit LPS-induced
399 nitric oxide production. *Pharm Biol.* 54, 1641–1648.
- 400
401 Liu, J.Y., Li, Y.H., Lin, H.X., Liao, Y.J., Mai, S.J., Liu, Z.W., Zhang, Z.L., Jiang, L.J., Zhang,
402 J.X., Kung, H.F., Zeng, Y.X., Zhou, F.J., Xie, D., 2013. Overexpression of YAP 1 contributes to
403 progressive features and poor prognosis of human urothelial carcinoma of the bladder. *BMC*
404 *Cancer.* 13,349. <http://doi.org/10.1186/1471-2407-13-349>
- 405
406 Madersbacher, S., Hochreiter, W., Burkhard, F., Thalmann, G.N., Danuser, H., Markwalder, R.,
407 Studer, U.E., 2003. Radical cystectomy for bladder cancer today—a homogeneous series without
408 neoadjuvant therapy. *J Clin Oncol.* 21, 690–696.
- 409
410 Neto-Silva, R.M., de Beco, S., Johnston, L.A., 2010. Evidence for a growth-stabilizing regulatory
411 feedback mechanism between Myc and Yorkie, the *Drosophila* homolog of Yap. *Dev Cell.* 19, 507–
412 520.
- 413
414 Ni, Z., Yao, C., Zhu, X., Gong, C., Xu, Z., Wang, L., Li, S., Zou, C., Zhu, S., 2017. Ailanthone
415 inhibits non-small cell lung cancer cell growth through repressing DNA replication via
416 downregulating RPA1. *Br J Cancer.* 117, 1621-1630.
- 417
418 No, J.H., Kim, Y.B., Song, Y.S., 2014. Targeting nrf2 signaling to combat chemoresistance. *J*
419 *Cancer Prev.* 19, 111-117.
- 420
421 Olayanju, A., Copple, I.M., Bryan, H.K., Edge, G.T., Sison, R.L., Wong, M.W., Lai, Z.Q., Lin,
422 Z.X., Dunn, K., Sanderson, C.M., Alghanem, A.F., Cross, M.J., Ellis, E.C., Ingelman-Sundberg,
423 M., malik, H.Z., Kitteringham N.R., Goldring, C.E., Park, B.K., 2015. Brusatol provokes a rapid
424 and transient inhibition of Nrf2 signaling and sensitizes mammalian cells to chemical toxicity-
425 implications for therapeutic targeting of Nrf2. *Free Radic Biol Med.* 78, 202–212.
- 426
427 Ren, D., Villeneuve, N.F., Jiang, T., Wu, T., Lau, A., Toppin, H.A., Zhang, D.D., 2011. Brusatol
428 enhances the efficacy of chemotherapy by inhibiting the Nrf2-mediated defense mechanism. *Proc*
429 *Natl Acad Sci U S A.* 108, 1433–1438.
- 430
431 Rojo de la Vega, M., Chapman, E., Zhang, D.D., 2018. NRF2 and the Hallmarks of Cancer. *Cancer*
432 *Cell.* pii: S1535-6108(18)30127-2. <https://doi.org/10.1016/j.ccell.2018.03.022>
- 433
434 Schneider, C.A., Rasband, W.S., Eliceiri, K.W., 2012. NIH Image to ImageJ: 25 years of image
435 analysis *Nat. Methods* 9, 671-675.
- 436
437 Shah, J.B., McConkey, D.J., Dinney, C.P., 2011. New strategies in muscle-invasive bladder cancer:
438 on the road to personalized medicine. *Clin Cancer Res.* 17, 2608–2612.
- 439
440 Sylvester, P.W., 2011. Optimization of the tetrazolium dye (MTT) colorimetric assay for cellular
441 growth and viability. *Methods Mol. Biol.*, 716, 157-168.
- 442
443 Tao, G., Kahr, P.C., Morikawa, Y., Zhang, M., Rahmani, M., Heallen, T.R., Li, L., Sun, Z., Olson,
444 E.N., Amendt, B.A., Martin, J.F., 2016. Pitx2 promotes heart repair by activating the antioxidant
445 response after cardiac injury. *Nature.* 534, 119-123.

446
61
62
63
64
65

- 447 Wang, R., Xu, Q., Liu, L., Liang, X., Cheng, L., Zhang, M., Shi, Q., 2016. Antitumour activity of 2-
448 dihydroailanthone from the bark of *Ailanthus altissima* against U251. *Pharm Biol.* 54, 1641–1648.
- 449
450 Warren, J.S.A., Xiao, Y., Lamar, J.M., 2018. YAP/TAZ Activation as a Target for Treating
451 Metastatic Cancer. *Cancers (Basel)*. 10(4), pii: E115. <http://doi.org/10.3390/cancers10040115>
- 452
453 Yu, W., Chen, Y., Dubrulle, J., Stossi, F., Putluri, V., Sreekumar, A., Putluri, N., Baluya, D., Lai,
454 S.Y., Sandulache, V.C., 2018. Cisplatin generates oxidative stress which is accompanied by rapid
455 shifts in central carbon metabolism. *Sci Rep.* 8(1),4306. <http://doi.org/10.1038/s41598-018-22640-y>
- 456
457 Zhang, C., Wang, H.J., Bao, Q.C., Wang, L., Guo, T.K., Chen, W.L., Xu, L.L., Zhou, H.S., Bian,
458 J.L., Yang, Y.R., Sun, H.P., Xu, X.L., You, Q.D., 2016. NRF2 promotes breast cancer cell
459 proliferation and metastasis by increasing RhoA/ROCK pathway signal transduction. *Oncotarget.* 7,
460 73593-73606.
- 461
462 Zhao, B., Ye, X., Yu, J., Li, L., Li, W., Li, S., Yu, J., Lin, J.D., Wang, C.Y., Chinnaiyan, A.M., Lai,
463 Z.C., Guan, K.L., 2008. TEAD mediates YAP-dependent gene induction and growth control.
464 *Genes Dev.* 22, 1962–1971.
- 465
466 Zhao, B., Li, L., Tumaneng, K., Wang, C.Y., Guan, K.L., 2010. A coordinated phosphorylation
467 by Lats and CK1 regulates YAP stability through SCF (beta-TRCP). *Genes Dev.* 24, 72–85.
- 468
469 Zhuo, Z., Hu, J., Yang, X., Chen, M., Lei, X., Deng, L., Yao, N., Peng, Q., Chen, Z., Ye, W.,
470 Zhang, D., 2015. Ailanthone Inhibits Huh7 Cancer Cell Growth via Cell Cycle Arrest and
471 Apoptosis In Vitro and In Vivo. *Sci Rep.* 5,16185. <http://doi.org/10.1038/srep16185>

472
473

474 **Figure legends**

475

476 *Figure 1.* MTT and colony forming assays in 253J B-V and 253J BV C-r cells. **Panel A:** MTT
477 assay. Results are expressed as percent of control values, obtained after 72 hours from the treatment
478 with the indicated concentrations of Aila or CDDP. Results are the mean \pm SD of four separate
479 experiments. $**p \leq 0.01$ vs sensitive cells. **Panel B:** Colony forming assay. Cells were treated with
480 the indicated concentrations of Aila or CDDP and cultured for 10 days.

481

482 *Figure 2.* MTT and colony forming assays in 253J and 253J C-r cells. **Panel A:** MTT assay.
483 Results are expressed as percent of control values, obtained after 72 hours from the treatment
484 with the indicated concentrations of Aila or CDDP. Results are the mean \pm SD of four separate
485 experiments. $**p \leq 0.01$ vs sensitive cells. **Panel B:** Colony forming assay. Cells were treated with
486 the indicated concentrations of Aila or CDDP and cultured for 10 days.

487

488 *Figure 3.* MTT and colony forming assays in T24 cells. **Panel A:** MTT assay. Results are expressed
489 as percent of control values, obtained after 72 hours from the treatment with the indicated
490 concentrations of Aila or CDDP. Results are the mean \pm SD of four separate experiments. **Panel B:**
491 Colony forming assay. Cells were treated with the indicated concentrations of Aila or CDDP and
492 cultured for 10 days.

493

494 *Figure 4. Panel A:* Western blot analysis of Nrf2, expression in 253J B-V, 253J BV C-r, 253J,
495 253J C-r and T24 cells in untreated (0) or treated with Aila at the indicated concentrations and
496 harvested after 24 or 48 hours. Equal protein loading was confirmed by exposure of the membranes

60

61

62

63

64

65

497 to the anti- β -actin antibody. Quantification of protein products was performed by densitometric
498 scanning. Data are normalized using the β -actin signal and are indicated as means \pm SD from three
499 independent experiments. **Panel B:** Quantification of protein products was performed by
500 densitometric scanning. Data were normalized using the β -actin signal and are indicated as the
501 mean \pm SD from three independent experiments. ** p-value ≤ 0.01 vs. untreated control cells (C).
502

503 *Figure 5. Panel A:* Western blot analysis of GSTA4 expression in 253J B-V, 253 J B-V C-r , 253J,
504 253J C-r and T24, untreated (0) or treated with Aila at the indicated concentrations and harvested
505 after 48h. Equal protein loading was confirmed by exposure of the membranes to the anti- α -tubulin
506 antibody. **Panel B:** Quantification of protein products was performed by densitometric scanning.
507 Data were normalized using the α -tubulin signal and are indicated as the mean \pm SD from three
508 independent experiments. ** p-value ≤ 0.01 and * p-value ≤ 0.05 vs. untreated control cells (C).
509

510 *Figure 6. Panel A:* Cell-cycle analysis in untreated (Control, C) or treated with 0.1 $\mu\text{g/ml}$ Aila
511 (0.1 Aila) or with 0.5 $\mu\text{g/ml}$ Aila (0.5 Aila) in 253J B-V and 253 J B-V C-r , at 24 hours. The data
512 were captured by using a BD Accuri Flow cytometer. Results were extracted and analysed by using
513 FCS Express Plus. Representative images and the relative percentages are shown. **Panel B:** Percent
514 of cell in cell cycle phases 24 hours after treatment with 0.1 $\mu\text{g/ml}$ Aila or 0.5 $\mu\text{g/ml}$ Aila in 253J B-
515 V and 253J B-V C-r. Data are the mean \pm SD of 3 separate experiments. ** $p \leq 0.01$, * $p \leq 0.05$ vs C.
516

517 *Figure 7. Panel A:* Western blot analysis of YAP and c-Myc expression in 253J B-V and 253J B-V
518 C-r cells untreated (0) or treated with Aila at the indicated concentrations and harvested after 24h
519 and 48 hours. Equal protein loading was confirmed by exposure of the membranes to the anti- β -
520 actin antibody. **Panel B:** Quantification of protein products was performed by densitometric
521 scanning. Data were normalized using the β -actin signal and are indicated as the mean \pm SD from
522 three independent experiments. ** p-value ≤ 0.01 vs. untreated control cells (C).
523

524 *Figure 8. Panel A:* wound healing assay at 0 (T0) and at 24 hours in 253J B-V and 253J B-V C-r
525 cells untreated (C) or treated with Aila at the indicated concentrations. **Panel B:** Quantification of
526 wound healing. The endpoint of the assay was measured by calculating the reduction in the width of
527 the wound after 24 hours and compared to T0 which is set at 100%. The data of each assay was
528 done from 3 independent experiments and shown as the mean \pm SD. ** $p \leq 0.01$ and * $p \leq 0.05$
529 vs. C.
530

531 *Figure 9.* Invasion assay at 24 hours in 253J B-V and 253J B-V C-r cells treated with Aila at the
532 indicated concentrations. Data are expressed as percentages of inhibition of cell invasion versus the
533 control invasion measured on untreated cells. The data of each assay was done from 5 independent
534 experiments and shown as the mean \pm SD. ** $p \leq 0.01$ and * $p \leq 0.05$ vs. C.
46
47
48
49
50
51
52
53
54
55
56
57
58
59
60
61
62
63
64
65

Figure 1
[Click here to download high resolution image](#)

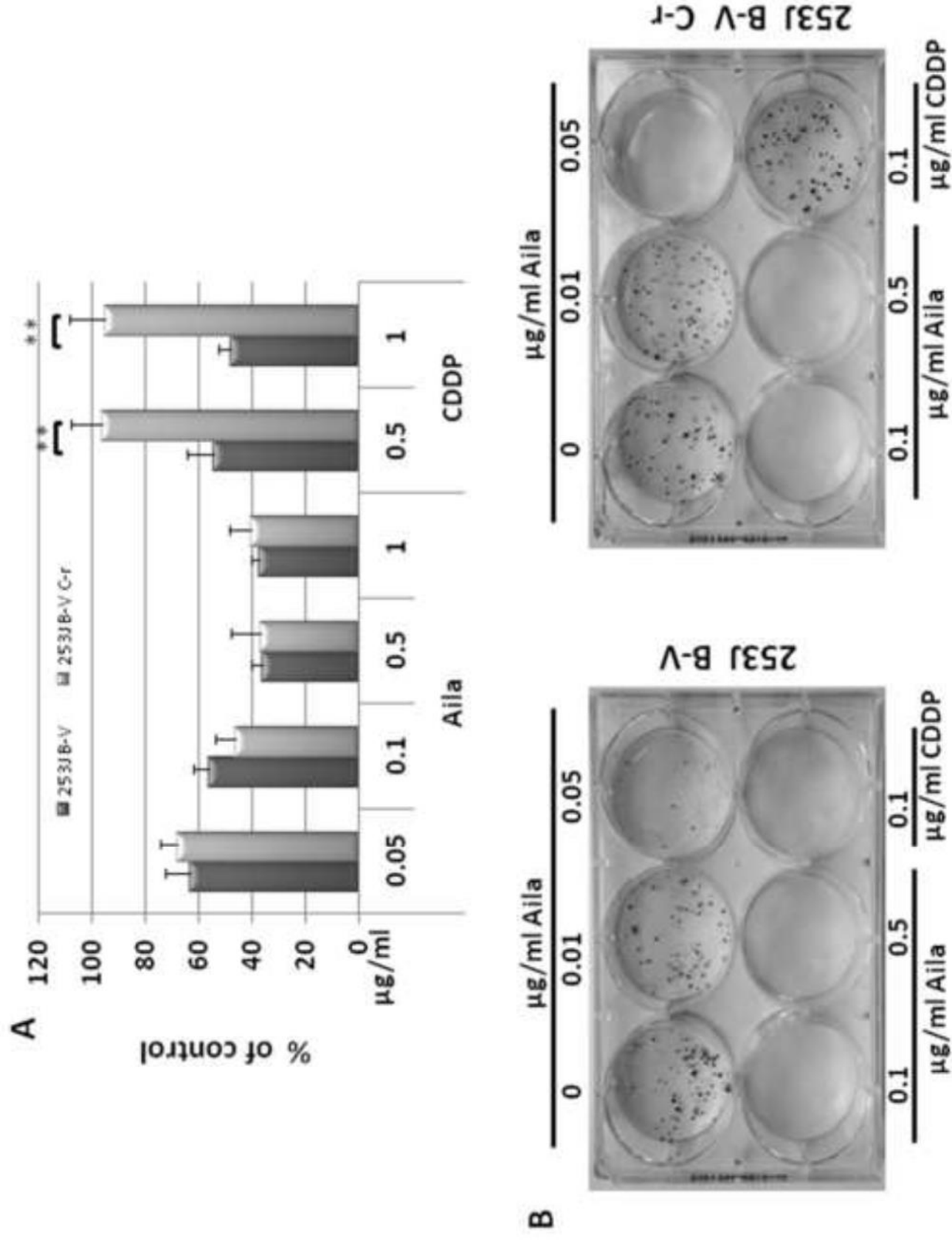


Figure 2
[Click here to download high resolution image](#)

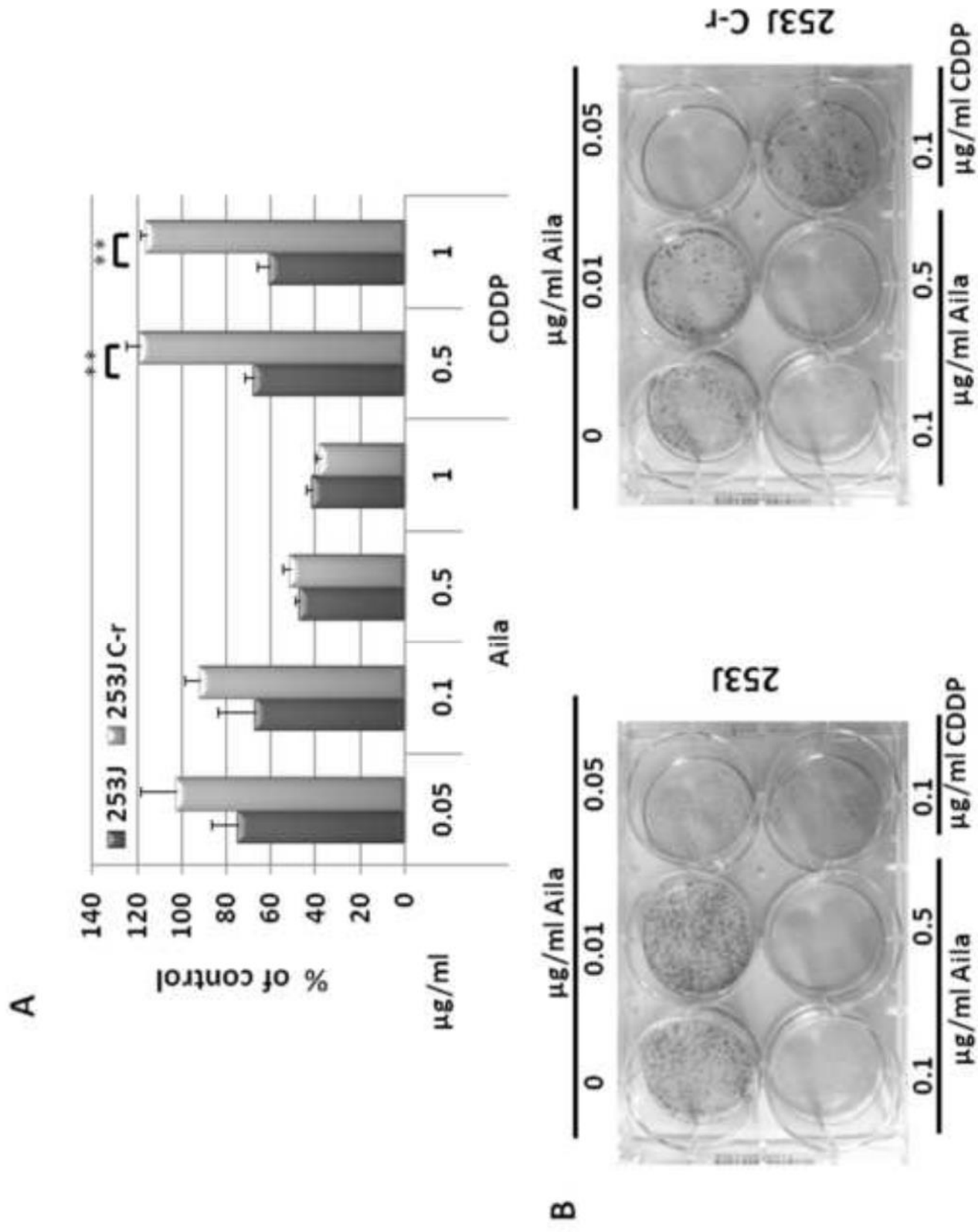


Figure 3
[Click here to download high resolution image](#)

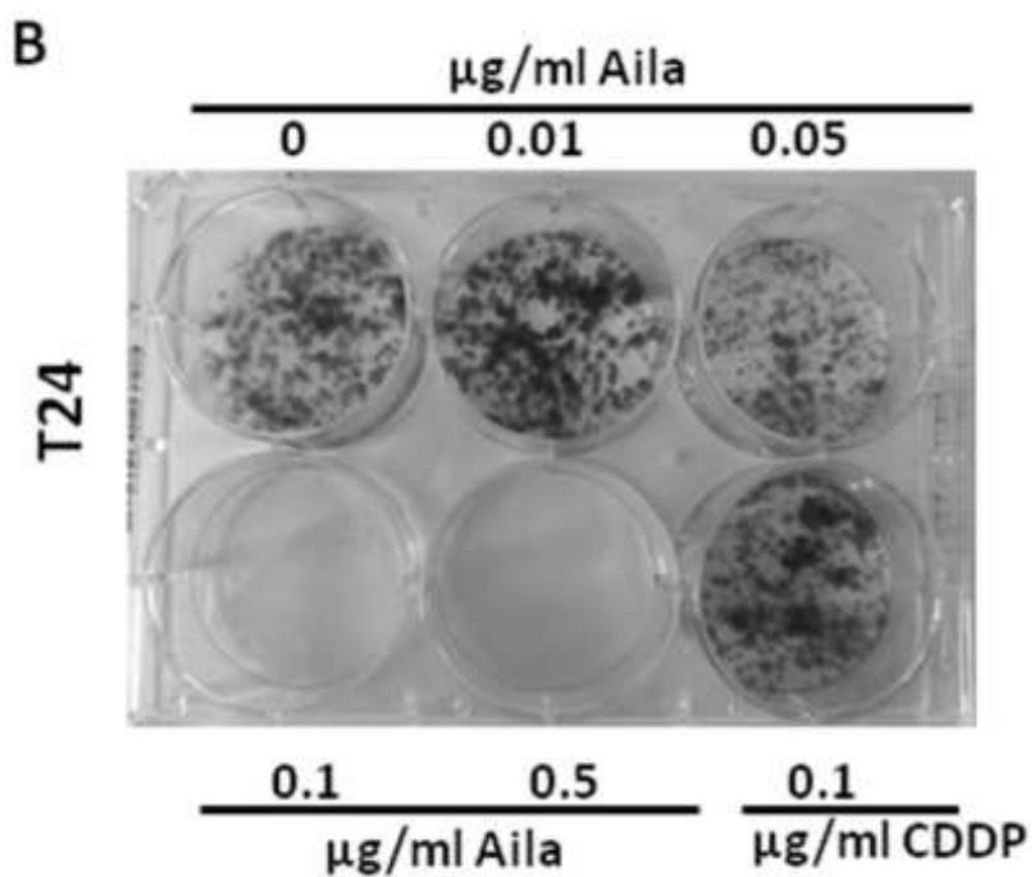
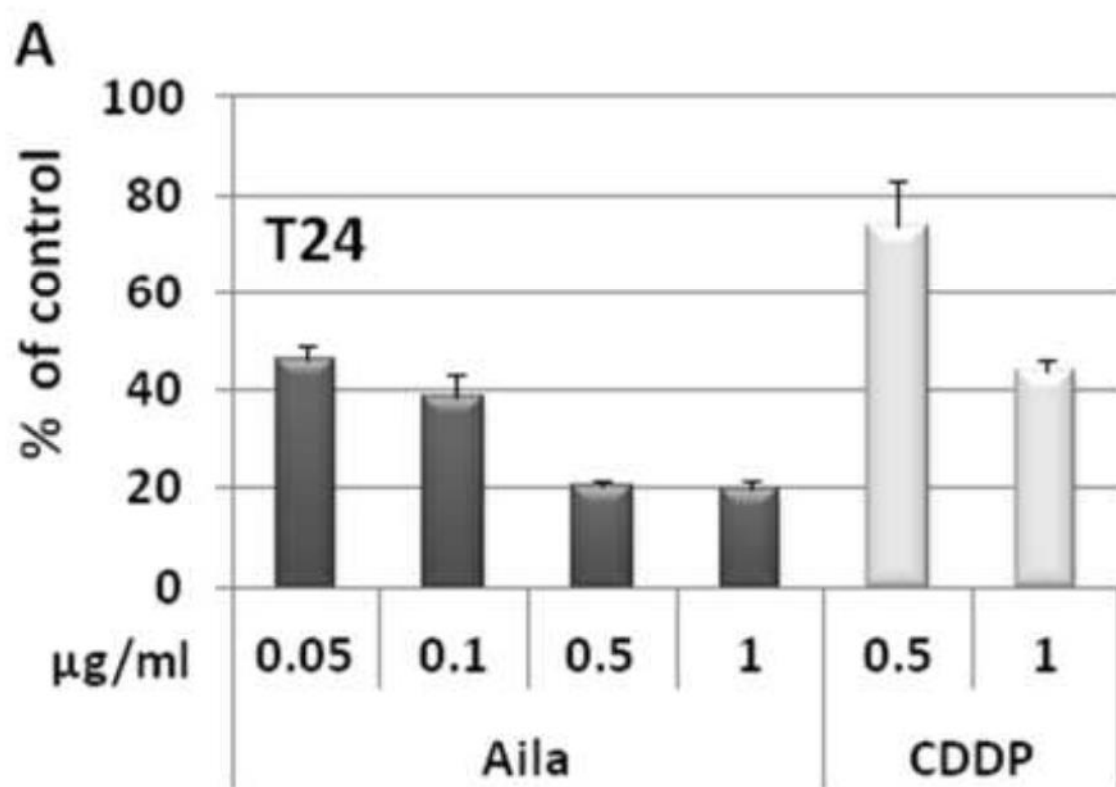
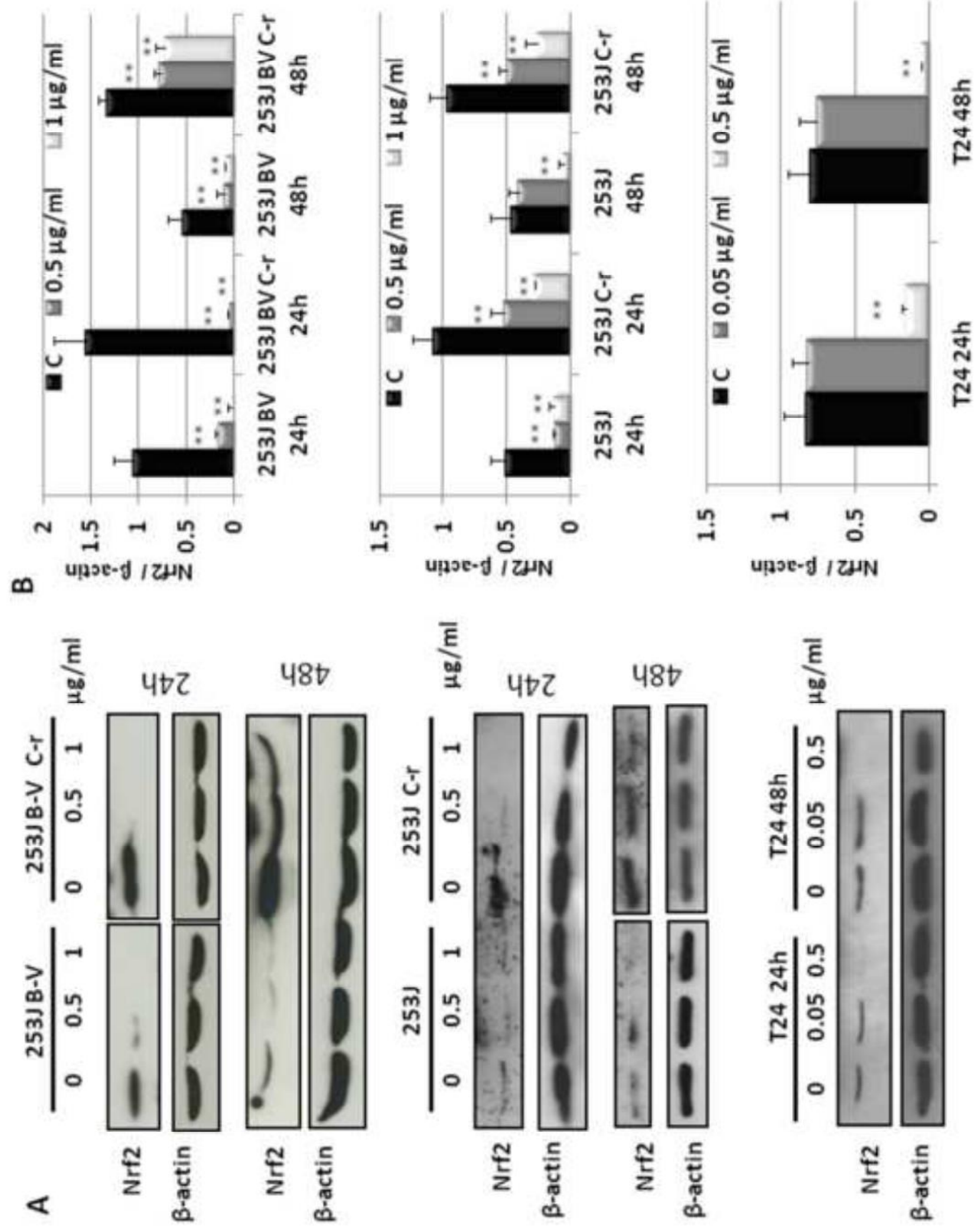


Figure 4
[Click here to download high resolution image](#)



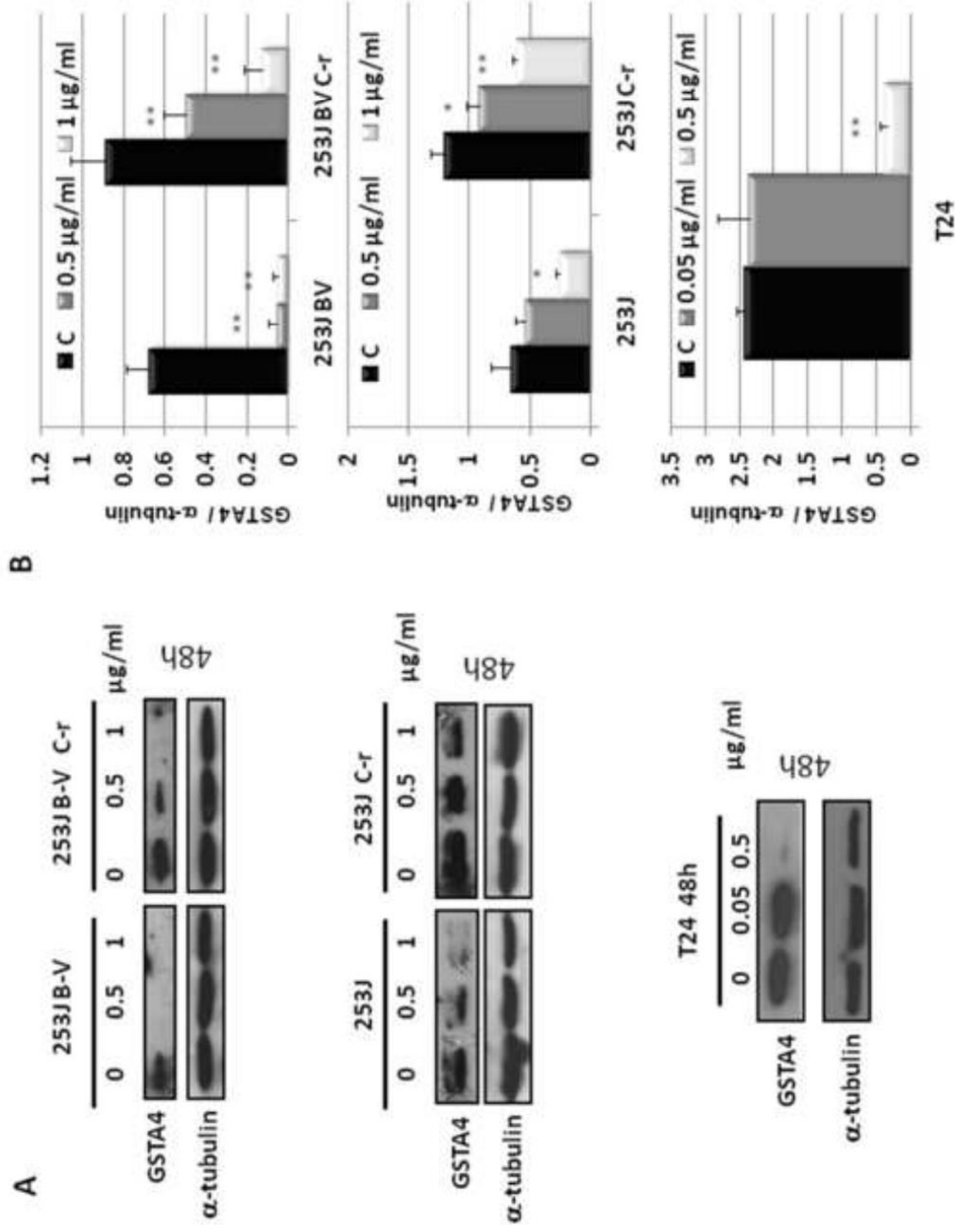
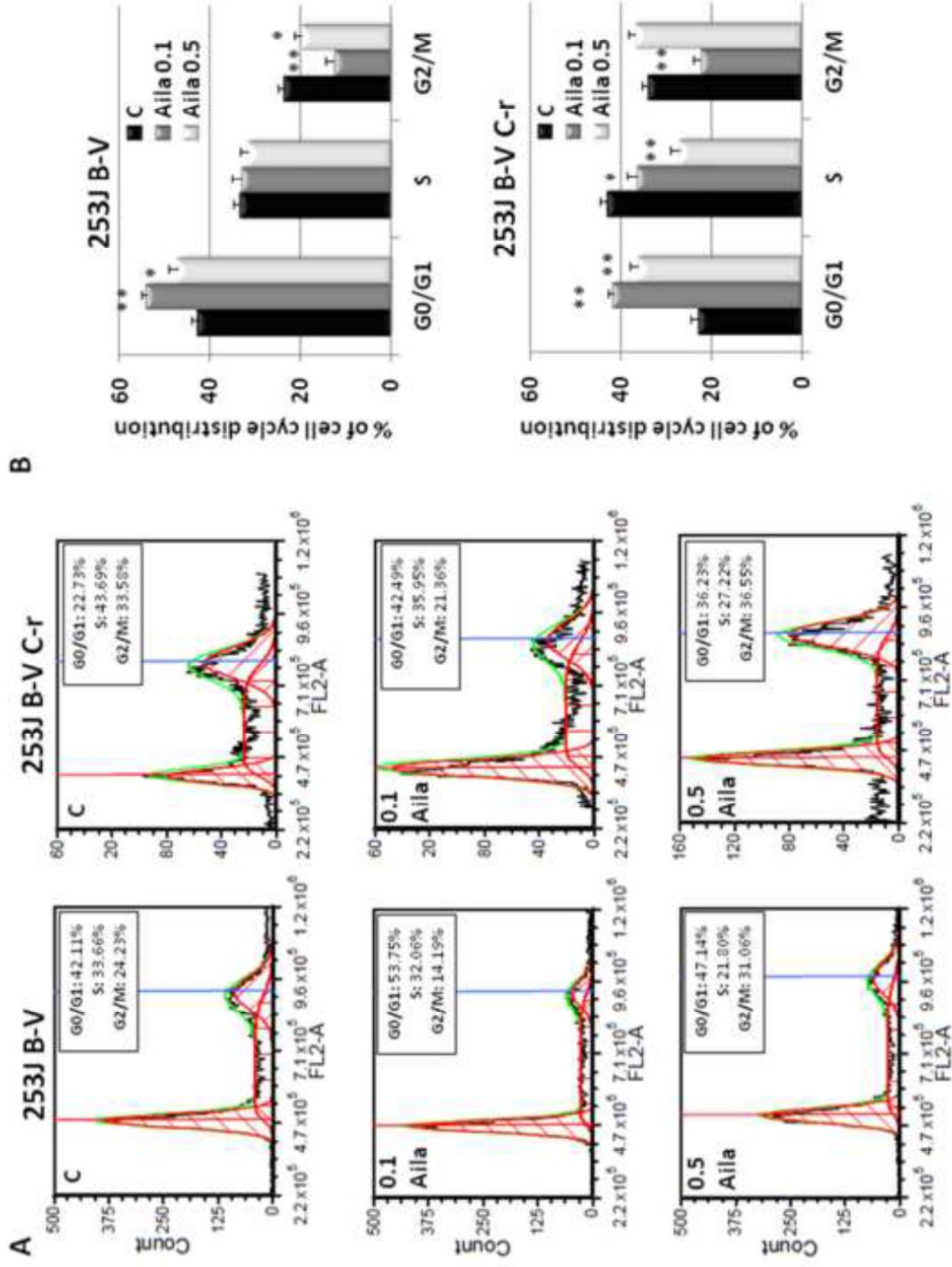


Figure 6
[Click here to download high resolution image](#)



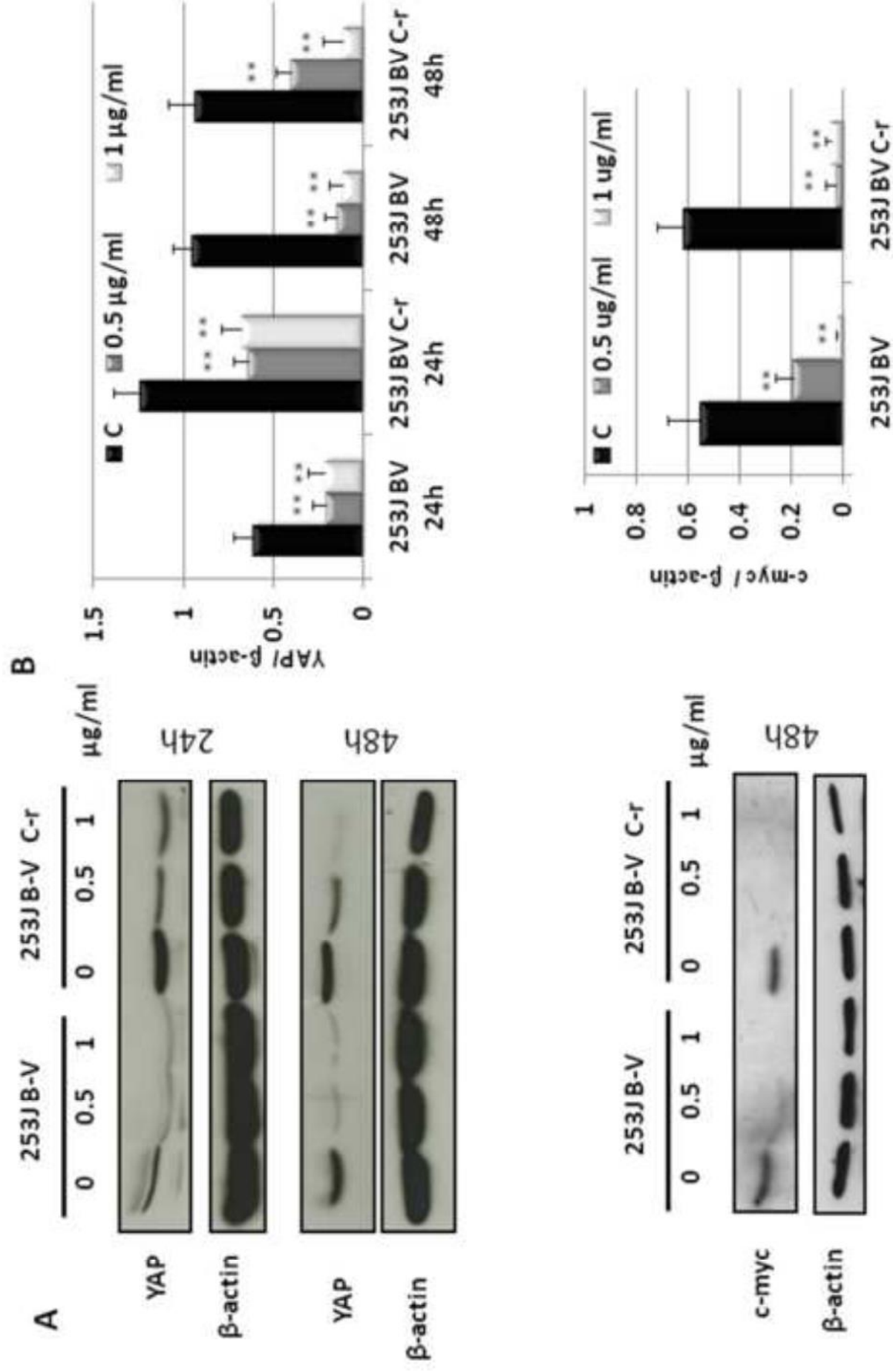


Figure 8
[Click here to download high resolution image](#)

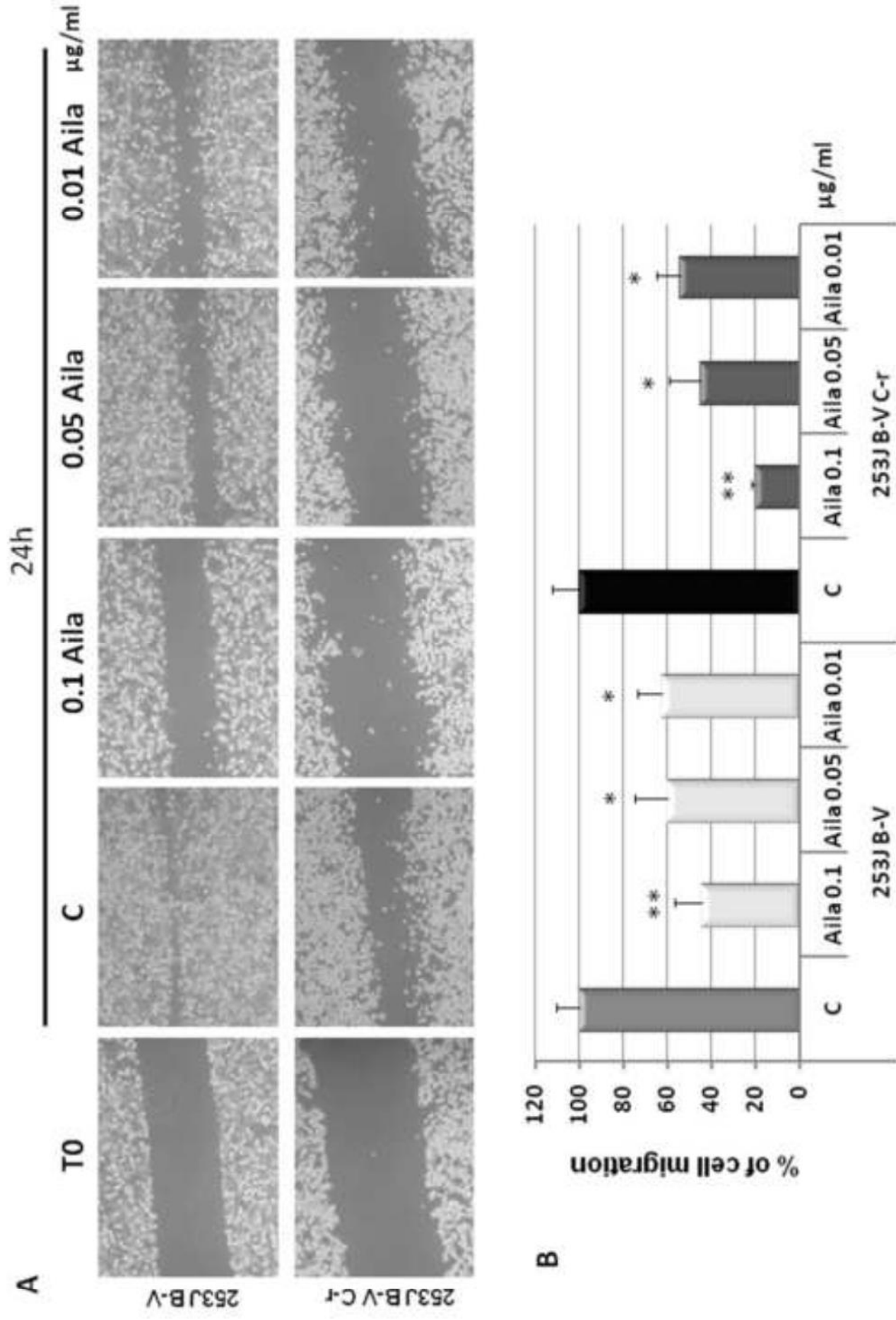


Figure 9
[Click here to download high resolution image](#)

